Received 23 March 2021; revised 5 May 2021; accepted 5 May 2021. Date of publication 11 May 2021; date of current version 19 May 2021.

Digital Object Identifier 10.1109/OJAP.2021.3079353

Reconfigurable Antennas Based on Pure Water

CHANGZHOU HUA [1] (Member, IEEE), SHIYAN WANG [2] (Member, IEEE), ZHENXIN HU [3] (Member, IEEE), ZEQI ZHU [3], ZHEN REN [4], WEN WU [4] (Senior Member, IEEE), AND ZHONGXIANG SHEN [5] (Fellow, IEEE)

(Invited Paper)

[1] Faculty of Electrical Engineering and Computer Science, Ningbo University, Ningbo 315211, China
[2] Jiangsu Key Laboratory of 3D Printing Equipment and Manufacturing, School of Electrical and Automation Engineering, Nanjing Normal University, Nanjing 210046, China
[3] School of Automation, Guangdong University of Technology, Guangzhou 510006, China
[4] School of Electronic and Optical Engineering, Nanjing University of Science and Technology, Nanjing 210094, China
[5] School of Electrical and Electronic Engineering, Nanyang Technological University, Singapore 639798

CORRESPONDING AUTHORS: C. HUA AND Z. SHEN (e-mail: huachangzhou@126.com; ezxshen@ntu.edu.sg)

This work was supported in part by the National Natural Science Foundation of China under Grant 61901125; in part by the State Key Laboratory of Millimeter Waves under Grant K202104; and in part by the Natural Science Foundation of Ningbo under Grant 2019A610071.

ABSTRACT This paper is concerned with the design of reconfigurable antennas based on pure water. Being a transparent, flexible, and readily available liquid, pure water can form a cylindrical stream that can be used to guide a leaky electromagnetic wave. By properly selecting the attenuation and phase constants of the leaky electromagnetic wave, the radiation characteristics of water antennas can be designed to suit different application requirements. By controlling the flow or size and shape of water, one can readily realize reconfigurable antennas of different operating frequencies, radiation patterns, and polarizations. Three novel antennas based on pure water are presented showing both simulated and measured results for their radiation performance. Topics that are worthwhile investigating in the future are also suggested.

INDEX TERMS Circular polarization, linear polarization, liquid antenna, reconfigurable antenna, water antenna.

I. INTRODUCTION

RECONFIGURABLE antennas have been extensively investigated in the past decade and many innovative designs have been proposed by numerous researchers [1], [2]. One or more of the radiation performances, such as the operating frequency, main direction, and polarization, of the radiated electromagnetic wave from reconfigurable antennas, can be adjusted to meet the growing demand for more wireless connection and compact size. Among a few mechanisms to implement an antenna's reconfigurability, the mechanical method has the advantages of exhibiting large tuning range and maintaining the antenna's good radiation performance after reconfiguration, though it has slow response compared to electrical switching. Liquid antennas [3]–[5] are an excellent candidate for designing reconfigurable antennas due to the fluidic nature of liquids. Numerous designs of liquid antennas including both liquid metals and liquid dielectrics have been proposed in the literature, and they exhibit excellent reconfigurability.

Water is a special liquid, which is naturally transparent, very flexible, and readily available. In addition, it exhibits a very high dielectric constant of around 80 at the room temperature. There has been a vast literature of water antennas [7]–[32] proposed by researchers around the world. Basically, they can be categorized into two types: sea-water antennas and pure-water antennas. Sea water can be considered as a good conductor at HF, VHF, and UHF bands. Therefore, a stream of sea surface. Both static and dynamic sea-water monopoles have been carefully studied and they can exhibit good radiation efficiency of above 50% at HF and VHF frequencies. Recent years have witnessed extensive attention on many antennas based on pure water, such as, dielectric resonator antennas [17], [20], [21], leaky-wave antenna [18], Yagi-Uda monopole [19], sea water can

be utilized as a radiating element for designing various antennas [7]–[16]. The most extensively studied sea-water antenna is the monopole antenna made of a vertical sea-water cylinder above either a metallic ground or an actual spiral antenna [22], [23], helical antenna [24], [25], hybrid monopole-dielectric resonator antenna [26]–[28], and patch antenna [29]–[31]. These pure-water antennas can be designed to be transparent and reconfigurable, as well as exhibiting very high radiation efficiency.

This paper presents a study of electromagnetic waves propagating along a cylindrical rod made of pure water. When the rod length is relatively short and comparable to the operating wavelength, standing-wave distribution of the electromagnetic field inside the water rod can be observed. However, when the rod length is several wavelengths long, a leaky traveling-wave can be excited inside the dielectric cylinder. By properly choosing the attenuation and phase constants of the leaky wave, suitable radiation characteristics can then be achieved. After that, three novel antennas based on pure water are described. After explaining these operating principles and design considerations, both simulated and measured results are provided, and they show very good agreement. They include a Vee antenna consisting of two tilted pure-water rods, a normal-mode helix antenna of circular polarization, and an array of several titled pure-water monopoles for producing omni-directional circular polarization. It has also been demonstrated that these antennas can be easily reconfigurable by adjusting the height of water filling in these rods. In Section IV, concluding remarks are made, along with several topics suggested for further investigation.

II. RADIATION PRINCIPLE OF PURE-WATER ANTENNA

The operating principle of the pure-water monopole, dipole, or long-wire antenna, etc. can be understood by studying electromagnetic waves propagating along a dielectric waveguide. It is well known that a dielectric rod or slab with a high dielectric constant can provide a wave-guiding boundary, similar to conductors. Therefore, the supported modes of a straight circular dielectric waveguide are hereby investigated to reveal the radiation principle of pure-water antennas.

The lowest order modes that a circular dielectric waveguide can excite are the HE_{11} mode and TM_{01} mode. The HE_{11} mode is the dominant mode and also the widely used operating mode of a circular dielectric waveguide, which has no cut-off frequency. However, the HE_{11} mode is difficult to be excited due to its asymmetric field distribution and may not be easily radiated out. As the frequency increases, the EM waves around the dielectric waveguide become more and more tightly bound. The next higher-order mode TM_{01} has a cut-off frequency f given by [32]:

$$f = \frac{2.405c}{\pi d\sqrt{\varepsilon_r - 1}} \tag{1}$$

where c represents the speed of light in free space, d stands for the diameter of the dielectric waveguide, ε_r is the relative permittivity of the dielectric. When the operating frequency approaches the cut-off of the TM_{01} mode, a frequency band appears, in which the electromagnetic wave will become "leaky" and can be radiated out well in the form of fast wave or leaky wave.

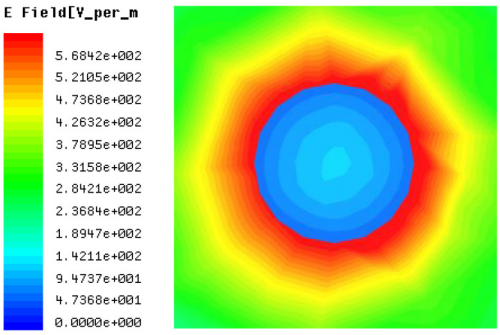

FIGURE 1. Electric field distribution at 1.5 GHz (cut-off state) in the cross-section plane of a center-fed circular pure-water waveguide.

In order to demonstrate the radiation principle, a center-fed circular pure-water waveguide is designed to excite the TM_{01} mode. Fig. 1 shows the electric field distribution at 1.5 GHz in the cross-sectional plane. It is clearly observed that a symmetric electric field appears, which reveals the excited axis-symmetrical mode. Besides, most of power is distributed in air since 1.5 GHz is lower than its cut-off frequency. According to equation (1), with the radius of the waveguide being 6 mm and the relative permittivity of pure water measured to be 78, the cut-off frequency can be calculated and it is equal to 2.18 GHz. The normalized phase constant (β/k_0) of the EM waves in the waveguide is extracted to compare with those of the metallic wire and waveguide, as shown in Fig. 2. The cross-section of the corresponding rectangular metallic waveguide is set to be 21×8 mm^2. It is seen that the normalized phase constant β/k_0 of a metallic wire is always equal to 1. As for the metallic rectangular waveguide, it is known that the supported modes propagate fast waves and their cut-off condition is:

$$\beta \leq 0 \tag{2}$$

In addition, it should be pointed out that the cut-off condition of a dielectric waveguide placed in air is:

$$\beta \leq k_0 \tag{3}$$

which is different from that of conventional metallic waveguide. It is also known that EM waves cannot effectively propagate in a waveguide when it is cutoff no matter whether it is a metallic waveguide or dielectric waveguide. However, for a metallic waveguide, the wave below cutoff is evanescent. For the dielectric one with open boundary, power is radiated into air because it would not damp with exponentially growing attenuation any more at the cut-off state [33]–[35]. It is found that the dielectric waveguide at cut-off state works in fast-wave status and possesses similar propagation characteristics to the transmission state of

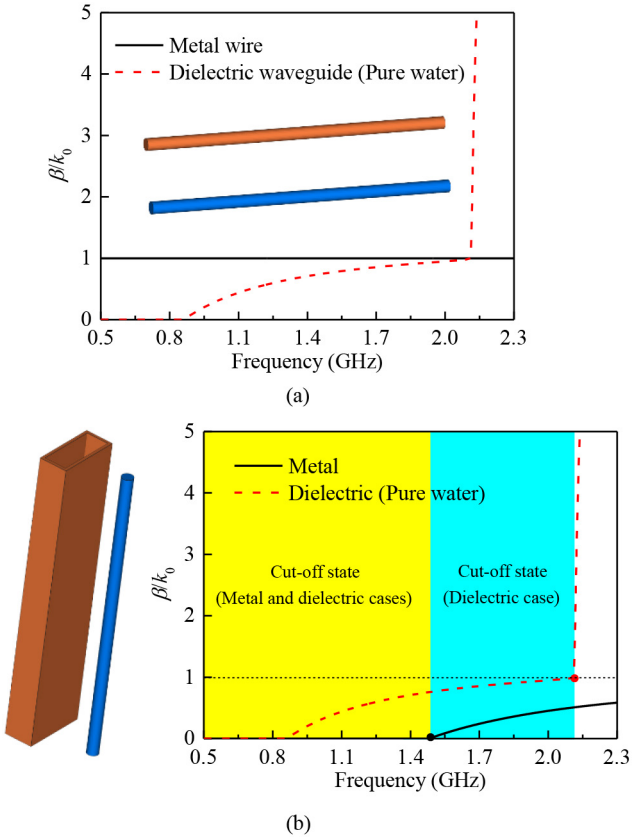

FIGURE 2. Comparison of normalized phase constant (β/k_0) between (a) Pure-water waveguide and metal wire. (b) Pure-water and metal waveguides.

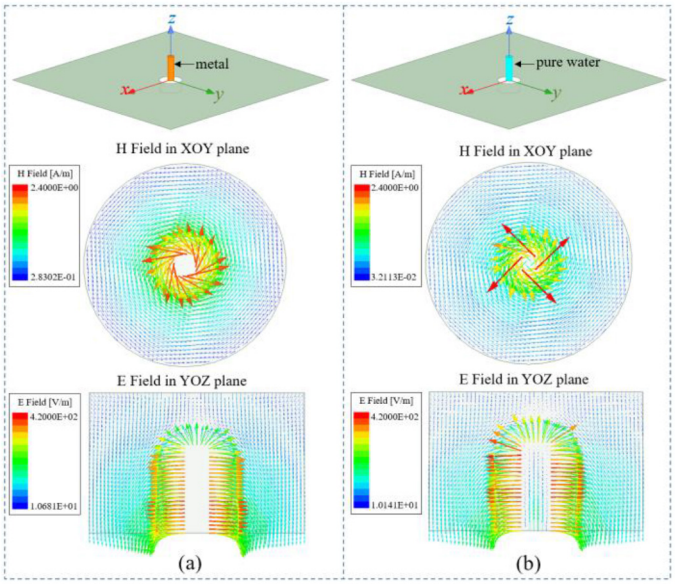

FIGURE 3. Field distributions of a coaxial-fed monopole antenna made of (a) metal, (b) pure water.

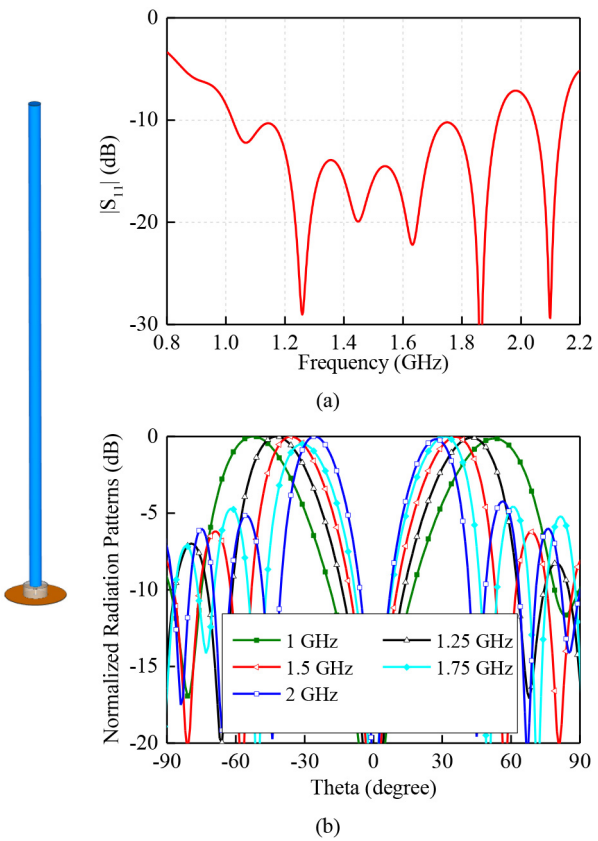

FIGURE 4. A study of long-wire dielectric antenna. (a) $|S_{11}|$. (b) Radiation pattern.

metallic waveguides although the power in dielectric can leak out into the air, which is intrinsically caused by the different boundaries. In the cut-off frequency range, the field distribution of a dielectric rod is very much like a PEC metallic rod, as shown in Fig. 3, where the field distributions of a metallic monopole antenna and pure-water monopole antenna are compared. The difference between these two cases is that there is no electric field inside the metallic rod due to the conductor's skin effect, but there is electric field inside the dielectric cylinder. If the concept of displacement current is introduced, the operating principle of the dielectric rod whether lossless or low loss is basically the same as that of the metallic rod. As a result, the traditional design method of the metallic monopole, dipole, or long-wire antennas, etc. can be used to design pure water antennas. Meanwhile, it can be expected that the radiation efficiency of this kind of pure water antenna will be very high as the loss tangent of pure water can be quite small.

A simple example of a long-wire dielectric antenna made of pure water is then provided to further verify the radiation principle, as shown in Fig. 4. On the one hand, the reflection coefficient reveals the traveling-wave impedance characteristic. On the other hand, the frequency-scanning property shown in its radiation pattern demonstrates the leaky-wave or fast-wave radiation. Furthermore, it is clearly observed that the antenna operates in the predicted frequency range of the cut-off state.

III. PURE-WATER VEE ANTENNA

Based on the radiation principle explained in the previous section, a pure-water Vee antenna is proposed to achieve

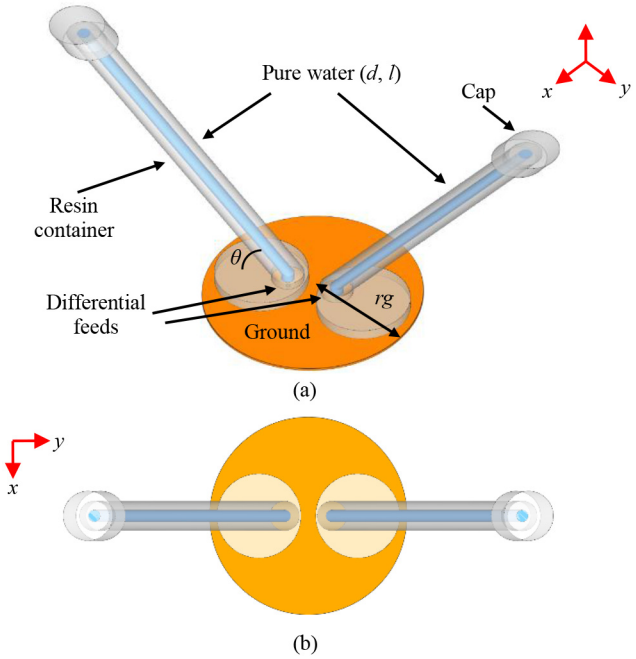

FIGURE 5. Configuration of the proposed pure-water Vee antenna. (a) 3-D view. (b) Top view. (d = 12 mm, l = 300 mm, rg = 100 mm, θ = 50°).

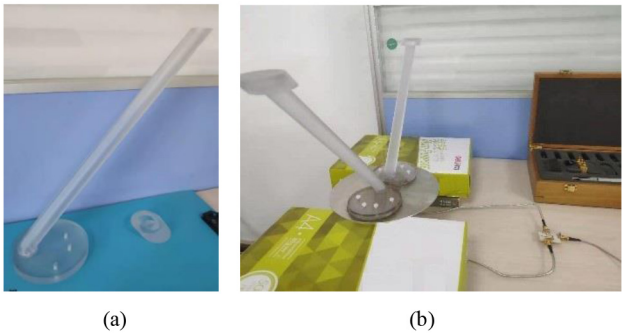

FIGURE 6. Fabricated antenna prototype. (a) 3-D printed resin container. (b) Antenna connected with a balun.

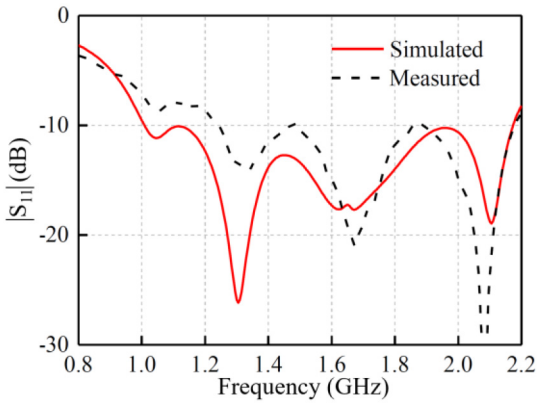

FIGURE 7. Comparison between the simulated and measured reflection coefficients versus frequency.

unidirectional radiation characteristics. It is known that a traditional Vee antenna made of metallic wires was developed to overcome the drawbacks of single long-wire antenna, such as low directivity and inclined beam. Besides, the wires of a Vee antenna must be nonresonant. Therefore, dielectric waveguide operating at the cut-off state and supporting traveling waves can be utilized to form a dielectric Vee antenna, thus achieving similar radiation performance to the metallic one. In addition, its radiation characteristics can be tuned due to the fluidic nature of pure water.

The configuration of the proposed pure-water Vee antenna is shown in Fig. 5. It is seen that the whole structure is the same as the metallic Vee antenna except for the resin container. As a kind of liquid, the pure water needs a transparent container to ensure its volume. The container with a pedestal is designed to support itself. A cap is also prepared to avoid the water leakage. Differential feeds are necessary for the Vee antenna and can be easily realized by employing a balun. The small ground is only used for impedance matching and does not seriously affect the radiation pattern of the antenna. In fact, the plane formed by the arms of the Vee antenna is parallel to the real ground plane in most applications [36]. As for the opening angle between the two arms of Vee antenna, it is desired to be relatively small for the maximum directivity.

Fig. 6 shows the fabricated antenna prototype. The water is filled in the 3-D printed resin container with transparency, which is made of Water Clear Ulter 10122, and the antenna is differentially fed by a coaxial line through a balun. The 2 mm-thick aluminum plate is fixed onto the container with several screws.

Fig. 7 depicts the simulated and measured reflection coefficients versus frequency. It is seen that the tendency of measured result is consistent with the simulated one. Although a relatively poorer impedance matching is observed in the low frequency, it is still applicable and may be improved in the future.

In addition, the operating frequency of our proposed Vee antenna can be reconfigurable, as seen from equation (1). Fig. 8 exhibits the simulated reflection coefficients when the diameter of the water arms is chosen to be 14, 12, and 10 mm, respectively. According to equation (1), the computed cut-off frequencies are 1.87, 2.18, and 2.62 GHz, respectively. They are in good agreement with the simulated ones of 1.88, 2.2, and 2.64 GHz seen in Fig. 8. Besides, the proposed antenna can be also reformed with reconfigurable polarization, as shown in Fig. 9. It is seen that the polarization of our antenna can be easily changed to an orthogonal direction by choosing the other pair of the arms.

The simulated and measured radiation patterns at 2 GHz are depicted in Fig. 9, which are in good agreement. As a common characteristic of Vee antenna, in the E-plane the designed antenna has two other beams beside the broadside-radiated one. In addition, it is worth mentioning that the measured gain is 7.1 dBi, which is quite high.

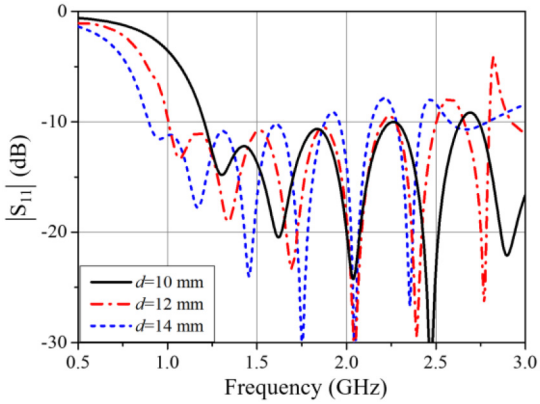

FIGURE 8. Simulated reflection coefficients for different diameters of water arms.

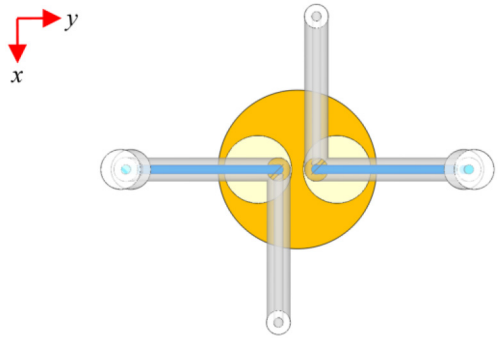

FIGURE 9. Reformed design of the proposed pure-water Vee antenna for polarization reconfigurability.

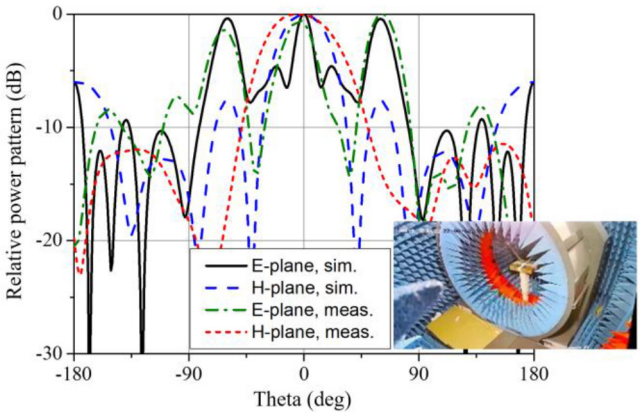

FIGURE 10. Comparison between the simulated and measured radiation patterns at 2 GHz.

IV. NORMAL-MODE WATER HELIX ANTENNA

Helical antennas are attractive in many wireless communication systems due to their simple structure, low cost, and excellent radiation performance. It is normally wounded using a thin metallic wire and can be described by a few parameters: diameter D, screw pitch S, and number of rolls n [37]. The radiation characteristics of the helical antenna basically depend on the ratio of helical diameter to the operating wavelength D/λ. There are basically two operating modes most frequently used: the normal mode and axial mode. When the diameter of the helix is small compared with the wavelength, the maximum radiation direction of the helical antenna is in the plane that is perpendicular to the spiral axis. It is a normal-mode helix and its parameters usually meet the following condition

$$D/\lambda < 0.18 \tag{4}$$

A normal-mode helix can be considered as the composition of loops with small diameters in the horizontal plane and short dipoles in the vertical plane, generating horizontally and vertically polarized E-field components, respectively. Specifically, a circular polarization (CP) can be achieved when D and S satisfy

$$\pi D = \sqrt{2S\lambda} \tag{5}$$

When the diameter gradually increases, the maximum radiation will change to the direction parallel to the axis of the helix. If the length of the helix for one roll is approximately one wavelength, circular polarization can also be obtained. Axial-mode helices can have broad bandwidth with CP radiation when

$$D/\lambda \approx 0.25 \sim 0.46 \tag{6}$$

Since the invention of helical antennas, metallic wires have been the principal material chosen to fabricate helix antennas. Dielectrics can hardly be found in the literature to be used for helical antennas. Recently, in [24], a helical antenna made of pure water is proposed. It was an axial-mode helical antenna made of pure water with a broad bandwidth and circular polarization. A reconfigurable topology was also presented in that work by combining two water pipes for producing two different polarizations.

In this section, a normal-mode CP water helical antenna is investigated. Fig. 11(a) shows the configuration of the water helical antenna. It consists of two water arms made of pure water and a transparent container to hold the water. The container is a 3-D printed structure using a dielectric material of dielectric constant around 3. The thickness of the container is 2 mm. The antenna is differentially fed at the center by a simple 3-D printed metallic balun. The helical antenna has a diameter of D, n turns and a screw pitch of S. Its cross-section has a rectangular shape with length L and width W.

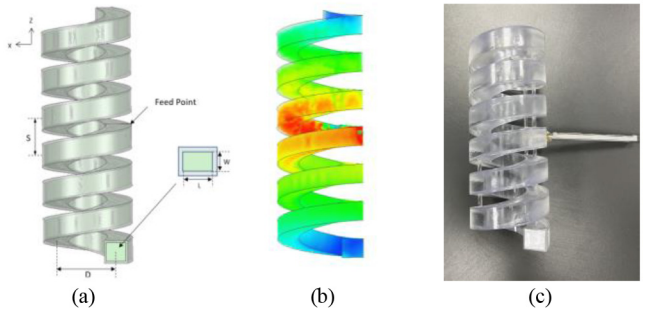

FIGURE 11. Water helical antenna. (a) Configuration. (b) Magnitude of E-Field inside the water. (c) Photo. (D = 48 mm, S = 28 mm, n = 6.2, L = 16 mm, W = 14 mm).

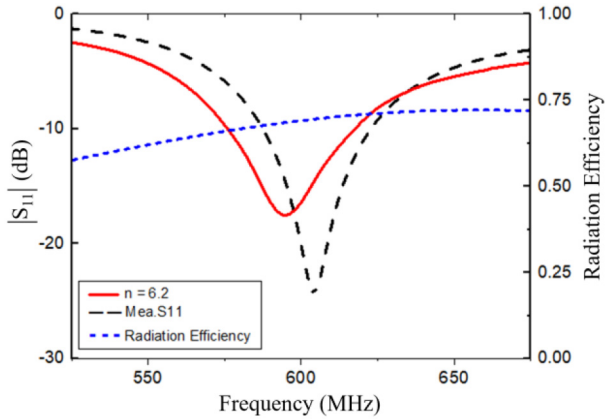

FIGURE 12. Simulated and measured reflection coefficient and simulated radiation efficiency of the water helical antenna.

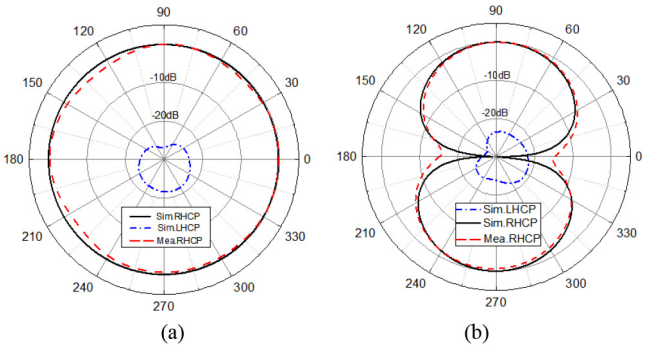

FIGURE 13. Simulated and measured normalized radiation patterns of the water helical antenna. (a) *xoy*-plane. (b) *xoz*-plane.

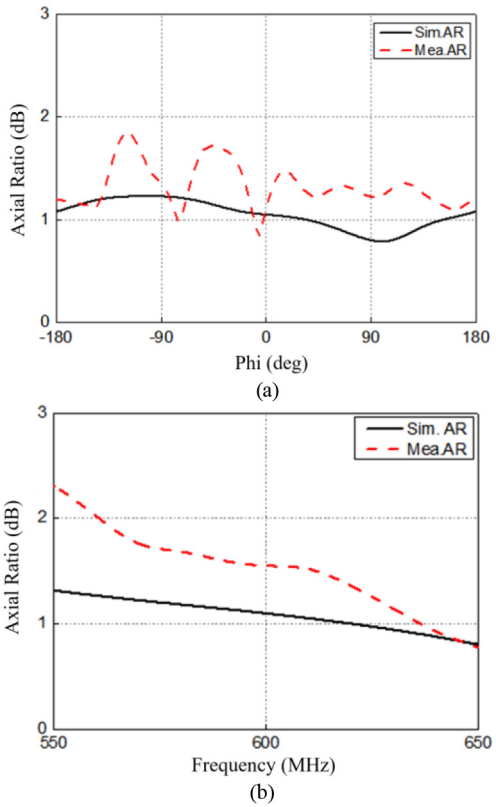

FIGURE 14. Simulated and measured AR of water helical antenna. (a) $f = 600$ MHz, $\theta = 90$ deg. (b) $\varphi = 90$ deg, $\theta = 90$ deg.

As discussed in Section II, the water arms can be considered as open dielectric waveguide. A guided wave can then be excited, traveling along the water arm. For the proposed normal-mode water helix, a quasi TM_{011} mode is excited considering the rectangular cross-section, while it should be TM_{01} mode for a circular cross-section. The total length of the water arms is about half a guided wavelength. The diameter D and screw pitch S still follow (5) for producing circular polarization.

The presented water helical antenna is designed to operate at around 600 MHz. The dielectric constant and loss tangent of the pure water are around $\varepsilon_r = 78.4$ and $\delta = 0.029$, respectively [38]. Fig. 11(b) shows the magnitude of the E-field distribution inside the water arms. The energy decays gradually along the propagation direction. Since the leakage constant is stable with an unchangeable cross-section, the radiated power should also gradually decrease along the propagation direction, which would result in an antenna aperture similar to a sinusoidal distribution. Fig. 11(c) shows a photo of the water helical antenna connected with a balun.

The simulated and measured reflection coefficient results of the water helical antenna are shown in Fig. 12. It can be seen the impedance bandwidth of the water helical antenna is from 585.3 MHz to 620.7 MHz (5.9%) for $|S11| < -10$ dB. The measured result is from 576 MHz to 616 MHz (6.7%), which is slightly wider than the simulated one. The simulated radiation efficiency of the water helical antenna is above 68% over the operating band.

The simulated and measured normalized radiation patterns are shown in Fig. 13. It can be seen that a pattern with a good roundness in the azimuth plane is obtained. The simulated gain is 0.9 dBic for RHCP and the measured one is 0.7 dBic. The cross-polarization is smaller than -22 dB in the azimuth plane. The simulated and measured axial ratio results of the proposed water helical antenna are shown in Fig. 14. It can be seen that the simulated axial ratio over the entire 360° range of the azimuth plane is lower than 3 dB with a very good average value of 1 dB. The measured result is slightly higher and more volatile than the simulated one, which may be due to the imperfect measurement setup and system error. Both the simulated and measured axial ratio results are smaller than 3 dB over a wide frequency range from 550 MHz to 650 MHz, showing that the proposed antenna has a wide AR bandwidth and stable CP performance.

In order to achieve a reconfigurable water helix, the glass container is divided into several segments with a thin glass wall between adjacent segments for isolation. The operating frequency can be tuned by filling up or emptying the containers, as shown in Fig. 15. The simulated reflection coefficients of the three different situations are shown in

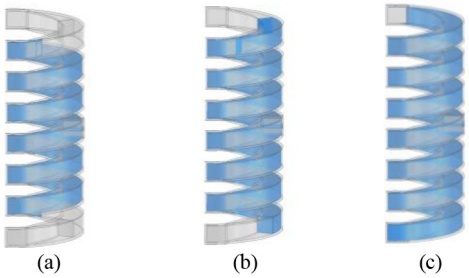

FIGURE 15. Configuration of the reconfigurable water helical antenna. (a) $n = 4.2$. (b) $n = 6.2$. (c) $n = 8.0$.

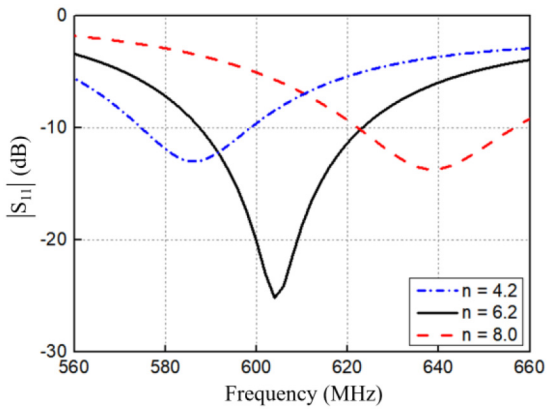

FIGURE 16. Simulated reflection coefficient of the reconfigurable water helical antenna.

Fig. 16. The operating frequency can be shifted in a broad frequency range from 585 MHz to 640 MHz maintaining a good circular polarization.

V. MONOPOLE ARRAY OF CIRCULAR POLARIZATION

In this section, a frequency-reconfigurable CP water monopole array is presented. Configuration of the proposed water monopole array is shown in Fig. 15. It consists of six elements and a circular ground plane with a diameter of D_m. It should be mentioned that no balun or phase shifters are needed. As shown in Fig. 15(b), the antenna element of the array is a tilted cylinder made of pure water with a length of l, a diameter of d and an inclination angle of α. The dielectric constant of pure water is measured to be 78.7 at the center frequency of 2 GHz. Transparent tubes made of acrylic are employed to hold the water. The dielectric constant of the acrylic is around 2.8, which is quite small compared with that of pure water. The thickness of the tubes is 1 mm. Each of the elements has a Teflon base with a diameter of d_b and height of h between the water cylinder and ground plane. Six coaxial probes are employed to stick into the water cylinders by a height of p to feed the elements. Fig. 17(c) shows the top view of the proposed monopole array. The water cylinders are uniformly distributed around the center of the ground plane. The distance between the center of the ground plane and each element is S. Detailed dimensions of the antenna are shown in Table 1. When all the six water elements are fed in-phase, a conical beam with left-hand circular polarization can be achieved. It should be mentioned that although left-hand circular polarization (LHCP) is obtained by the proposed antenna, right-hand circular polarization (RHCP) can also be readily obtained by tuning each of the element by 180°.

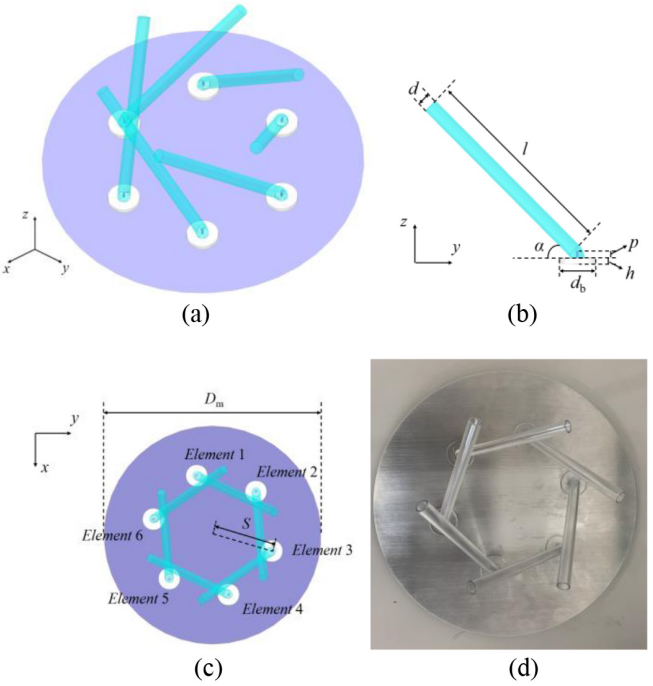

FIGURE 17. Configuration of the proposed water monopole array. (a) Perspective view, (b) Element, (c) Top view. (d) Photo. ($D_m = 300$ mm, $S = 110$ mm, $d = 8$ mm, $l = 130$ mm, $p = 4$ mm, $h = 1$ mm, $d_b = 20$ mm, $\alpha = 50°$).

TABLE 1. Dimensions of the proposed water monopole array.

Parameter	D_m	S	d	l	p
Value	300 mm	110 mm	8 mm	130 mm	4 mm
Parameter	h	d_b	α		
Value	1 mm	20 mm	50°		

By controlling the water volume, the length l of the water cylinder elements can be changed and the operating frequency of the antenna can then be tuned. Fig. 18 shows the simulated and measured reflection coefficient and axial ratio results of the proposed monopole array with different values of l. When $l = 130$ mm, an axial ratio lower than 3 dB is obtained from 1.7 GHz to 2.15 GHz and the impedance bandwidth for $|S_{11}| < -10$ dB is 21.3% from 1.8 GHz to 2.23 GHz, which means the proposed water monopole array achieves a wideband stable CP performance. When l is changed, the operating band of axial ratio changes as well. It can be seen that by changing the length of the water element, the operating frequency of the antenna can be tuned covering a wide range.

Simulated and measured radiation patterns of the proposed monopole array with different values of l at different frequencies are shown in Fig. 19. It can be seen that the radiation pattern is stable when the antenna's operating

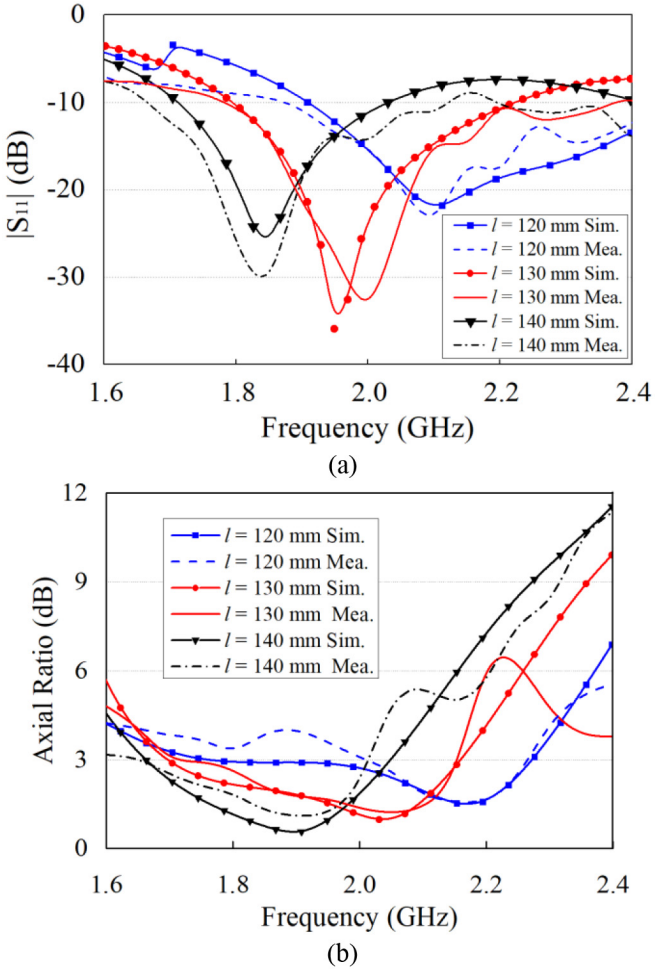

FIGURE 18. Simulated and measured results of (a) reflection coefficient and (b) axial ratio of the water monopole array with different *l*.

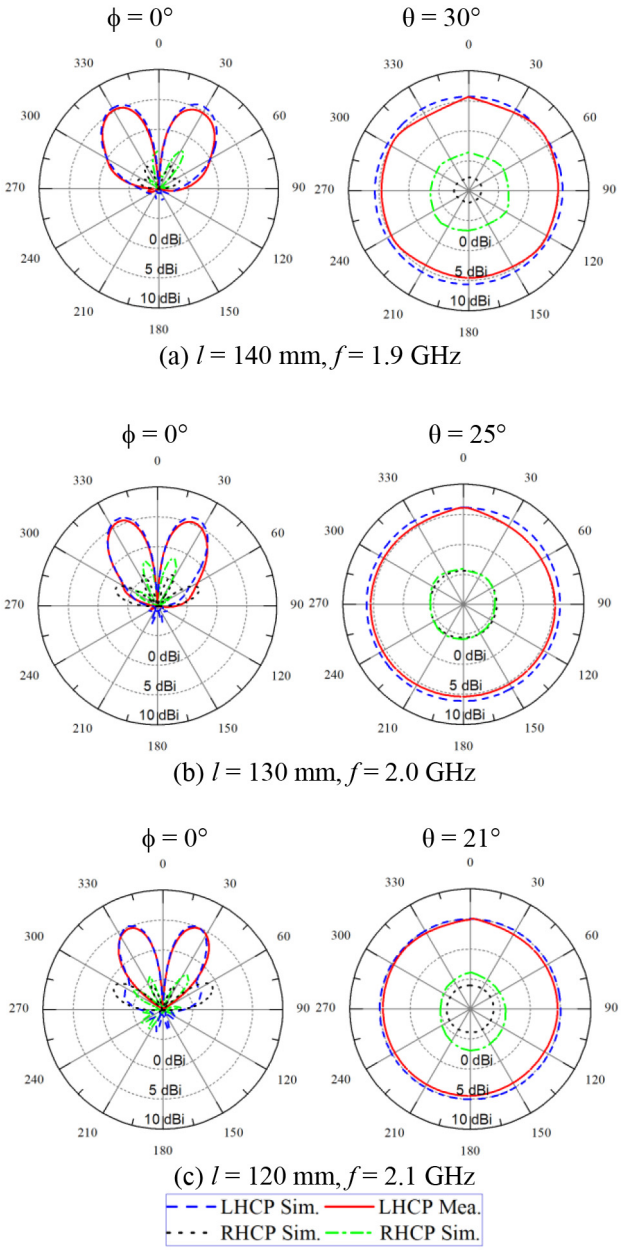

FIGURE 19. Simulated and measured radiation patterns of the water monopole array.

frequency is tuned. A conical beam with good roundness and a maximum gain of 6.1 dBic for LHCP is obtained. The pointing-angle of the conical beam when $l = 130$ mm at 2.0 GHz is 25°. Cross-polarization lower than −10 dB is obtained over the entire 360° range around the azimuth plane.

When the six elements fed by the coaxial probes with different phases, the radiation performance of the proposed water monopole array can be quite different. When Elements 1 to 6 shown in Fig. 17 are fed with 0°, 60°, 120°, 180, 240° and 300°, a conical beam with linear polarization is achieved. The axial ratio of the proposed water monopole array working in LP state is shown in Fig. 20. The axial ratio is higher than 12.5 dB at 2 GHz, indicating a linear polarization. Fig. 21 shows the simulated radiation patterns of the monopole array working in LP state. It can be seen that a conical beam with a pointing angle of 33° and good roundness is obtained. A maximum gain of 5.8 dBi for LP is achieved as well.

When Elements 1 to 6 shown in Fig. 17 are fed with 0°, −60°, −120°, −180, −240° and −300°, a pencil beam with LHCP can be achieved. Axial ratio of the array working in this pencil beam state is shown in Fig. 22. It can be seen that an axial ratio lower than 3 dB is obtained from 1.75 GHz to 2.36 GHz. Simulated radiation pattern is shown in Fig. 23, and a pencil-beam with a maximum gain of 6.9 dBic is obtained.

VI. CONCLUDING REMARKS

This paper has presented a detailed design of several reconfigurable antennas based on pure water. The radiation principle and main design considerations of antenna made of pure-water rod have been investigated, which demonstrates that a pure-water rod can provide a wave-guiding medium, similar to a metallic rod, within a certain frequency

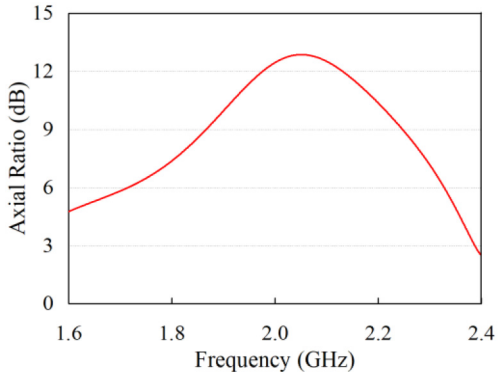

FIGURE 20. Simulated axial ratio of the water monopole array working in LP state.

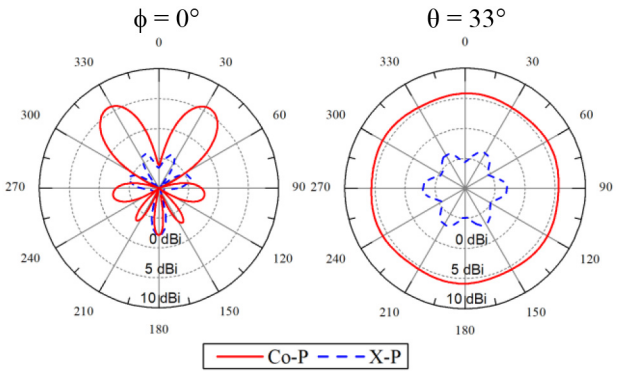

FIGURE 21. Simulated radiation patterns of the water monopole array working in LP state.

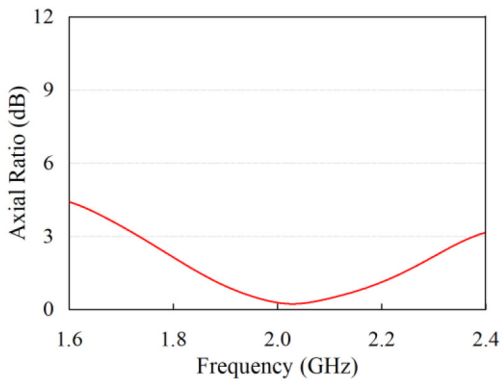

FIGURE 22. Simulated axial ratio of the water monopole array working in pencil-beam state.

range. It is highlighted that the operating frequency of the water antenna should be below the cut-off frequency range of the intended mode of the dielectric waveguide. After that, three pure-water rod antennas, include pure-water Vee antenna, normal-mode helix antenna, and circularly-polarized monopole antenna array, have been designed, fabricated, and measured. Simulated and measured results show very good agreement, which exhibits that pure water can be used as a good radiator. Meanwhile, it has also been shown that these antennas can be easily made reconfigurable by adjusting the height of water filling in these

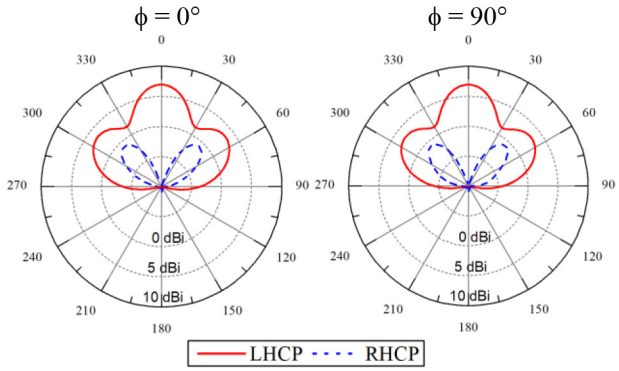

FIGURE 23. Simulated radiation patterns of the water monopole array working in pencil-beam state.

rods. The main features of these pure-water antennas include their high transparency, reconfigurability, low cost, and simple structures. All these characteristics make these antennas potentially very useful for future wireless communications.

It is worth mentioning that although the tunable mechanism of these pure-water antennas is not involved in this paper, there are many tunable methods [39]–[42]. One way is that we can follow the liquid reconfigurable system in [41] to control the height of water filling in the pure-water rods by using a microfluid pump and mechanical switches. Another way to dynamically reconfigure the pure-water antenna is by using the temperature control method, due to the temperature dependence of the permittivity and loss tangent of water [42].

There may be other antennas that can be designed based on pure water. Due to its transparent and fluidic nature, pure water can be employed to design radar antennas that can exhibit very low radar cross section, while they can also be reconfigurable. This is very attractive and deserves extensive investigation. On the other hand, water antennas can be potentially very useful in the ubiquitous Internet of Things applications that are being introduced now and in the near future. While water antennas can be used to provide the necessary wireless connectivity, they may also serve as visual decorations if they are artistically shaped and elegantly designed. In addition, other innovative water antennas may also be designed for medical applications [43] and orbital angular momentum systems [44].

REFERENCES

[1] R. L. Haupt and M. Lanagan, "Reconfigurable antennas," *IEEE Antennas Propag. Mag.*, vol. 55, no. 1, pp. 49–61, Feb. 2013.

[2] J. Constantine, Y. Tawk, S. E Barbin, and C. G. Christodoulou, "Reconfigurable antennas: Design and applications," *Proc. IEEE*, vol. 103, no. 3, pp. 424–437, Mar. 2015.

[3] M. Zou, Z. Hu, C. Hua, and Z. Shen, "Liquid antennas," in *Wiley Encyclopedia of Electrical and Electronics Engineering*. Chichester, U.K.: Wiley, Nov. 2016.

[4] Y. Kosta, "Liquid antenna," in *IEEE AP-S Int. Symp. Dig.*, vol. 3, Jun. 2004, pp. 2392–2395.

[5] H. Fayad and P. Record, "Broadband liquid antenna," *Electron. Lett.*, vol. 42, no. 3, pp. 133–134, 2006.

[6] E. Paraschakis, H. Fayad, and P. Record, "Ionic liquid antenna," in *Proc. IEEE Int. Workshop Antenna Technol. Small Antennas Novel Metamater.*, 2005, pp. 552–554.
[7] D. W. S. Tam, "Electrolytic fluid antenna with signal enhancer," U.S. 8 368 605 B1, 2009.
[8] L. Xing, Y. Huang, S. S. Alja'afreh, and S. J. Boyes, "A monopole water antenna," in *Proc. Loughborough Antennas Propag. Conf.*, 2012, pp. 1–4.
[9] C. Hua, Z. Hu, and Z. Shen, "Reconfigurable water antennas," in *Proc. IEEE Int. CAMA Conf.*, 2014, pp. 1–2.
[10] C. Hua, Z. Shen, and J. Lu, "High-efficiency sea-water monopole antenna for maritime wireless communications," *IEEE Trans. Antennas Propag.*, vol. 62, no. 12, pp. 5968–5973, Dec. 2014.
[11] C. Hua and Z. Shen, "Shunt-excited sea-water monopole antenna of high efficiency," *IEEE Trans. Antennas Propag.*, vol. 63, no. 11, pp. 5185–5190, Nov. 2015.
[12] C. Hua and Z. Shen, "Sea-water half-loop antenna for maritime wireless communications," in *Proc. IEEE 4th APCAP Conf.*, 2015, pp. 231–232.
[13] L. Xing, Y. Huang, Q. Xu, S. Aljáafreh, and T. Liu, "A broadband hybrid water antenna for hand-portable applications," *IEEE Antennas Wireless Propag. Lett.* vol. 15, pp. 174–177, 2016.
[14] S. Wang, Z. Hu, W. Wang, and S. Qi, "Analysis and design of sea-water monopole Yagi-Uda antenna with pattern reconfigurability," *Int. J. RF Micow. Comput. Aided Eng.*, vol. 28, no. 12, Apr. 2018, Art. no. e21399.
[15] X. Pan, Z. Hu, M. Zheng, Z. Ren, and Q. Chen, "A UHF sea-water array antenna for maritime wireless communications," in *Proc. 12th Eur. Conf. Antennas Propag.*, 2018, p. 670.
[16] Q. Yang, B. Yuan, and Y. Suo, "Research on simulation and calculation of a novel ultra-wideband reconfigurable salt-water antenna," in *Proc. Int. Symp. Antennas Propagation (ISAP)*, Xi'an, China, 2019, pp. 1–3.
[17] R. Zhou, H. Zhang, and H. Xin, "A compact water based dielectric resonator antenna," in *IEEE AP-S Int. Symp. Dig.*, Jun. 2009, pp. 1–4.
[18] Z. Hu, Z. Shen, and W. Wu, "Reconfigurable leaky-wave antenna based on periodic water grating," *IEEE Antennas Wireless Propag. Lett.* vol. 13, pp. 134–137, 2014.
[19] Z. Hu, W. Wu, Z. Shen, and C. Hua, "A Yagi monopole antenna made of pure water," in *Proc. IEEE AP-S Int. Symp. (APS/URSI)*, Jul. 2015, pp. 2241–2242.
[20] M. Zou, Z. Shen, and J. Pan, "Frequency-reconfigurable water antenna of circular polarization," *Appl. Phys. Lett.*, vol. 108, no. 1, Jan. 2016, Art. no. 14102.
[21] M. Zou, Z. Shen, and J. Pan, "Frequency-reconfigurable water dielectric resonator antenna," in *Proc. 17th Int. Symp. Antenna Technol. Appl. Electromagn. (ANTEM)*, 2016, pp. 1–4.
[22] Z. Hu, S. Wang, Z. Shen, and W. Wu, "Broadband polarization - reconfigurable water spiral antenna of low profile," *IEEE Antennas Wireless Propag. Lett.* vol. 16, pp. 1377–1380, 2017.
[23] G. Li, G. Gao, Z. Tian, and W. Liu, "Tunable and flexible liquid spiral antennas," *IET Electron. Lett.*, vol. 53, no. 10, pp. 648–650, 2017.
[24] Z. Ren, S.-S. Qi, Z. Hu, Z. Shen, and W. Wu, "Wideband water helical antenna of circular polarization," *IEEE Trans. Antennas Propag.* vol. 67, no. 11, pp. 6770–6777, Nov. 2019.
[25] Z. Ren, S. Qi, W. Wu, and Z. Shen, "Reconfigurable RHCP-to-LP helical antenna made of pure water," in *Proc. IEEE Int. Symp. Antennas Propag. USNC-URSI Radio Sci. Meeting*, 2019, pp. 457–458.
[26] Y.-H. Qian and Q.-X. Chu, "A broadband hybrid monopole-dielectric resonator water antenna," *IEEE Antennas Wireless Propag. Lett.* vol. 16, pp. 360–363, Jun. 2016.
[27] M. Wang and Q.-X. Chu, "High-efficiency and wideband coaxial dual-tube hybrid monopole water antenna," *IEEE Antennas Wireless Propag. Lett.* vol. 17, no. 5, pp. 799–802, Mar. 2018.
[28] L. Xing, J. Zhu, Q. Xu, D. Yan, and Y. Zhao, "A circular beam-steering antenna with parasitic water reflectors," *IEEE Antennas Wireless Propag. Lett.* vol. 18, no. 10, pp. 2140–2144, Oct. 2019.
[29] Y. Li and K.-M. Luk, "A water dense dielectric patch antenna," *IEEE Access*, vol. 3, pp. 274–280, 2015.
[30] J. Sun and K.-M. Luk, "A wideband low cost and optically transparent water patch antenna with omnidirectional conical beam radiation patterns," *IEEE Trans. Antennas Propag.*, vol. 65, no. 9, pp. 4478–4485, Sep. 2017.
[31] J. Sun and K.-M. Luk, "A Wideband and optically transparent water patch antenna with broadside radiation pattern," *IEEE Antennas Wireless Propag. Lett.*, vol. 19, no. 2, pp. 341–345, Feb. 2020.
[32] C. L. Chen, *Foundations for Guided-Wave Optics*. Hoboken, NJ, USA: Wiley, 2006.
[33] D. Marcuse, *Theory of Dielectric Optical Waveguides*. New York, NY, USA: Academic Press, 1974.
[34] J. R. James, "Theoretical investigation of cylindrical dielectric rod antennas," *Proc. Inst. Electr. Eng.*, vol. 114, no. 3, pp. 309–319, Mar. 1967.
[35] S. Wang *et al.*, "Radar cross-section reduction of helical antenna by replacing metal with 3D printed zirconia ceramic," *IEEE Antennas Wireless Propag.*, vol. 19, no. 2, pp. 350–354, Feb. 2020.
[36] C. A. Balanis, *Antenna Theory: Analysis and Design*. Hoboken, NJ, USA: Wiley, 2005.
[37] J. D. Kraus and R. J. Marhefka, *Antennas For All Applications*, 3rd ed. New York, NY, USA: McGraw-Hill, 2002.
[38] T. Meissner and F. J. Wentz, "The complex dielectric constant of pure and sea water from microwave satellite observations," *IEEE Trans. Geosci. Remote Sens.*, vol. 42, no. 9, pp. 1836–1849, Sep. 2004.
[39] X. Xie *et al.*, "High-efficiency and tunable circular-polarization beam splitting with a liquid-filled all-metallic catenary meta-mirror," *Adv. Mater. Technol.*, vol. 4, no. 7, Jun. 2019, Art. no. 900334.
[40] K. Entesari and A. P. Saghati, "Fluidics in microwave components," *IEEE Microw. Mag.*, vol. 17, no. 6, pp. 50–75, Jun. 2016.
[41] L. Xing *et al.*, "A high-efficiency wideband frequency reconfigurable water antenna with a liquid control system," *IEEE Antennas Propag. Mag.*, vol. 63, no. 1, pp. 61–70, Feb. 2021.
[42] A. T. Mobashsher and A. Abbosh, "Reconfigurable water-substrate based antennas with temperature control," *Appl. Phys. Lett.*, vol. 110, no. 25, Jun. 2017, Art. no. 253503.
[43] Y. Jin, J. Tak, and J. Choi, "Broadband hybrid water antenna for ISM-band ingestible capsule endoscope systems," in *Proc. Int. Workshop Antenna Technol. (iWAT)*, 2016, pp. 82–85.
[44] J. Ming and Y. Shi, "A mode reconfigurable orbital angular momentum water antenna," *IEEE Access*, vol. 8, pp. 89152–89160, 2020.

CHANGZHOU HUA (Member, IEEE) was born in Zhejiang, China, in 1984. He received the B.S. degree in electronics information engineering and the Ph.D. degree in communication engineering from the Nanjing University of Science and Technology, Nanjing, China, in 2007 and 2013, respectively.

He was a Visiting Researcher with the Department of Information and Electronic Engineering, Zhejiang University, Hangzhou, China, from 2009 to 2012. From 2013 to 2015, he was with the School of Electrical and Electronic Engineering, Nanyang Technological University, Singapore, as a Research Fellow. He joined the Faculty of Electrical Engineering and Computer Science, Ningbo University, Ningbo, China, in March 2015. From October 2017 to December 2017, he was a Visiting Associate Professor with the State Key Laboratory of Terahertz and Millimeter Waves, City University of Hong Kong, Hong Kong. He has authored or coauthored more than 50 journal papers and conference papers. His current research interests include liquid antennas, reconfigurable antennas, filtering antennas, and lens antenna.

SHIYAN WANG (Member, IEEE) received the B.Eng. and Ph.D. degrees from the Nanjing University of Science and Technology, Nanjing, China, in 2014 and 2019, respectively.

From 2017 to 2018, he joined as a Research Assistant with the University of Macau, Macau, China. He is currently with the School of Electrical and Automation Engineering, Nanjing Normal University. His research interests include microstrip patch antenna, liquid antenna, dielectric antenna, and 3-D printing technology.

ZHENXIN HU (Member, IEEE) was born in Xuzhou, China, in 1988. He received the B.S. degree in detection, guidance, and control technology and the Ph.D. degree in electromagnetic field and microwave technology from the Nanjing University of Science and Technology, Nanjing, China, in 2011 and 2016, respectively.

He was a Research Assistance with the School of Electrical and Electronic Engineering, Nanyang Technological University, Singapore, from 2012 to 2015. He served with Antenna Business Group, Huawei Technologies Company Ltd. from 2016 to 2018. He is currently with the School of Automation, Guangdong University of Technology. His research interests include reconfigurable water antennas, high-impedance helical antennas, multiband dual-polarized base station antenna arrays, wideband low-profile antennas with endfire radiation, and Terahertz spectroscopy.

ZEQI ZHU was born in Shantou, China, in 1996. She received the B.S. degree from the School of Automation, Guangdong University of Technology, Guangzhou, China, in 2020, where she is currently pursuing the M.S. degree in control engineering. Her research interests include reconfigurable helical water antennas.

ZHEN REN was born in China, in 1990. He received the B.Eng. degree in electronic and technology engineering from Xidian University, Xi'an, China, in 2012. He is currently pursuing the Ph.D. degree in information and communication engineering with the Nanjing University of Science and Technology.

His current research interests include the design of water antennas and reconfigurable antennas.

WEN WU (Senior Member, IEEE) received the Ph.D. degree in electromagnetic field and microwave technology from Southeast University, Nanjing, China, in 1997.

He is currently a Professor with the School of Electronic and Optical Engineering, and an Associate Director with the Ministerial Key Laboratory of JGMT, Nanjing University of Science and Technology, Nanjing. He has authored and coauthored over 90 journal and conference papers, and has held eight patents. His research interests include integrated circuits, antennas, microwave and millimeter-wave theories and technologies, microwave and millimeter-wave detection, and multimode compound detection.

Prof. Wu has received six times of the Ministerial and Provincial-Level Science and Technology Awards.

ZHONGXIANG SHEN (Fellow, IEEE) received the B.Eng. degree in electrical engineering from the University of Electronic Science and Technology of China, Chengdu, China, in 1987, the M.S. degree in electrical engineering from Southeast University, Nanjing, China, in 1990, and the Ph.D. degree in electrical engineering from the University of Waterloo, Waterloo, ON, Canada, in 1997.

From 1990 to 1994, he was with the Nanjing University of Aeronautics and Astronautics, Nanjing. In 1997, he joined Com Dev Ltd., Cambridge, ON, Canada, as an Advanced Member of Technical Staff. In 1998, he joined the Gordon McKay Laboratory, Harvard University, Cambridge, MA, USA, and the Radiation Laboratory, University of Michigan at Ann Arbor, Ann Arbor, MI, USA, as a Postdoctoral Fellow. In 1999, he joined Nanyang Technological University, Singapore, as an Assistant Professor, where he is currently a Full Professor. He has authored or coauthored more than 200 journal papers (among them 140 were published in IEEE journals) and presented more than 180 conference papers. His current research interests include the design of small and planar antennas for various wireless communication systems, analysis and design of frequency-selective structures, and hybrid numerical techniques for modeling RF/microwave components and antennas.

Prof. Shen served as the Chair for the IEEE MTT/AP Singapore Chapter in 2009. He was the Chair of the IEEE AP-S Chapter Activities Committee from 2010 to 2014. He is currently an Associate Editor of the IEEE Transactions on Antennas and Propagation. He served as the Secretary of the IEEE AP-S from July 2014 to December 2018, and he was an elected AdCom Member of the IEEE AP-S from January 2016 to December 2019.